



Electrosynthesis of Polyaniline on Carbon Fiber Felt: Influence of Voltammetric Cycles on Electroactivity

Anne Karoline dos Santos Poli,^a Gustavo Machado Domingues Caetano,^{b,c}
Ludmila Resende Vargas,^a Adriana Medeiros Gama,^b Maurício Ribeiro Baldañ,^{a,d}
and Emerson Sarmiento Gonçalves^{a,b,z}

^aInstituto Tecnológico da Aeronáutica, Praça Marechal Eduardo Gomes, 12228-900 São José dos Campos, SP, Brazil

^bInstituto de Aeronáutica e Espaço, Laboratório de Caracterização Físico-Química, Divisão de Materiais, Praça Marechal Eduardo Gomes, 12228-904 São José dos Campos, SP, Brazil

^cETEP Faculdades, 12000-000 São José dos Campos, SP, Brazil

^dInstituto Nacional de Pesquisas Espaciais, Laboratório Associado de Sensores, 12227-010 São José dos Campos, SP, Brazil

The carbon materials and conducting polymers are known by application in electronic devices. This work aims to study the initial steps parameters of polyaniline electrosynthesis on carbon felts annealed at 1600 K by changing the number of voltammetry cycles in aniline acid solution. The characterization was performed by Field Emission Gun – Scanning Electron Microscopy, X-ray Diffraction, Infrared Fourier Transform Spectroscopy, Raman Spectroscopy and Electrochemical Impedance Spectroscopy. Under increasing number of cycles, the growth was more intense and it was easy to observe the pores clogging. Besides, it was noticed that emeraldine formation occurred progressively, from structures less to more oxidized: the polyaniline less cycled resulted closest to leucoemeraldine; polyaniline from nine cycles resulted closest to emeraldine, but all of them showed electroactive defects related to electrical charge (polarons) and conductivity (bipolarons). It was also observed that prime layers of polyaniline, formed until three cycles, followed more intense attraction of charges in solution to layer surface. This effect was emphasized from 3rd to 6th cycles. © 2017 The Electrochemical Society. [DOI: 10.1149/2.1521709jes] All rights reserved.

Manuscript submitted May 24, 2017; revised manuscript received July 7, 2017. Published July 20, 2017.

Development of radar absorbing materials (RAM) or storage energy devices highlighted in last decades due to increasing challenges related to military strategies, aerospace requirements, and shortage of energy sources, telecommunication improvements and environmental questions. In this context, conducting polymers has been reported as material applied to assembly these devices. Besides, it is very important to obtain composites that shows suitable electrochemical, mechanical and thermal properties,^{1,2} when exposed to electromagnetic field in several frequency bands.^{3,4}

Several methods to obtain these polymers are reported in literature, specially involving chemical or electrochemical synthesis.¹ Chemical synthesis is a high yield process but it is less manageable and it produces several byproducts and wastes, specifically to polyaniline (PANI), one of the most investigated conducting polymers. In the other hand, electrosynthesis is cleaner and more controllable than chemical synthesis, although generates lower yields. In this paper, electrosynthesis has been chosen due to great redox activity especially when acid doped, it is a versatile material for electronic application.² In fact, for a material to be used in electronic and aerospace devices, the relationship between electrode specific mass and electrochemical activity or electromagnetic field interaction is an important parameter, where both parameters must be achieved with a minimum material specific mass. In such materials obtained with this end, it is very important to choose a substrate useful in these areas. If the substrate has to be maintained in the electrode structure, then the choice of a slight, porous and high surface area material is extremely important.³ These properties are easily found in carbon electrodes, which have been intensively studied as electrode materials for energy storage applications such as batteries and supercapacitors.² Furthermore, it is a material with a great potential to apply to prevent electromagnetic interferences (EMI).⁴

Nunzianto and Pistoia⁵ also found significant differences in the voltammetric profiles when PANI films are grown at different sweep rates. Furthermore, Cui et al.⁶ discussed the origin of the difference between potentiostatic and cyclic potential sweep methods to deposit polyaniline. The cyclic voltammetric films were shown to have morphological and adhesion properties making them suitable for practical purposes. The same authors have also shown⁷ that the morphology of PANI films obtained by cyclic voltammetry from HClO₄ solutions

is a function of the scan rate, the rotation speed of the working electrode, the number of deposition cycles and the aniline concentration. Andrade et al.⁸ showed that, for PANI films grown using linear potential sweep technique, the rate of only the first cycle was an important factor to control the morphology and therefore the electrical properties of the polymer films.

In conducting polymers, different to other materials, charge carriers are electrons or holes located in bandgap, and characterized as charges strongly associated to structure defects. During oxidation, solutions are formed as polaron or bipolaron. In case of polaron, a cation radical formed when an electron moves from valence band to approximately middle of bandgap.⁶ Furthermore, polaron has spin associated to lattice deformation.⁹ Parallel to this approach, it is very common to work with a molecular analysis, which considers the role of polarons and bipolarons on resonance phenomena in polymer chain. Polarons distort locally a cluster of neighbor atoms, through generation of electron-hole pair, with bond breaking. After oxidation, double bonds at PANI backbone are broken, remaining at radical cation at chain, a **polaron**. When a second electron is removed from polymeric chain, its abstraction from polaron is thermodynamically favored in relation to from other point of chain (in whose case would there be two polarons). In this case, it is generated a bipolaron, a dication associated to more stable local defect. Stable bipolaron formation is related to energy gain by interaction with lattice is greater than coulombian repulsion between two confined charges of same signal.¹⁰ Emeraldine salt is electric conducting, because polarons can move at π backbone, such as, if PANI has bipolarons, there is interaction between non-neighbor atoms in polymer chain. This property increases density of states, providing higher conductivity and electrochromism.

Because formation of these phonons (polarons and bipolarons), important functional composition changes of PANI are associated to a broad variety of oxidation states, determined by doping degree. To PANI, oxidation forms are: leucoemeraldine (combination of reduced repetitive units, $y = 0$); emeraldine (combination between reduced and oxidized half units, benzenoid and quinoid forms, respectively, $y = 0.5$), which have potential to be the more conductive form; and pernigraniline (where all units are composed by totally oxidized units, $y = 1$). This parameter y represents the number of anions inserted in a repetitive unit of polymer. Therefore, the y informs about the oxidation degree of the PANI molecule. This information used when Raman Scattering Spectroscopy analyzes the material for this

^zE-mail: sarmgon@yahoo.com

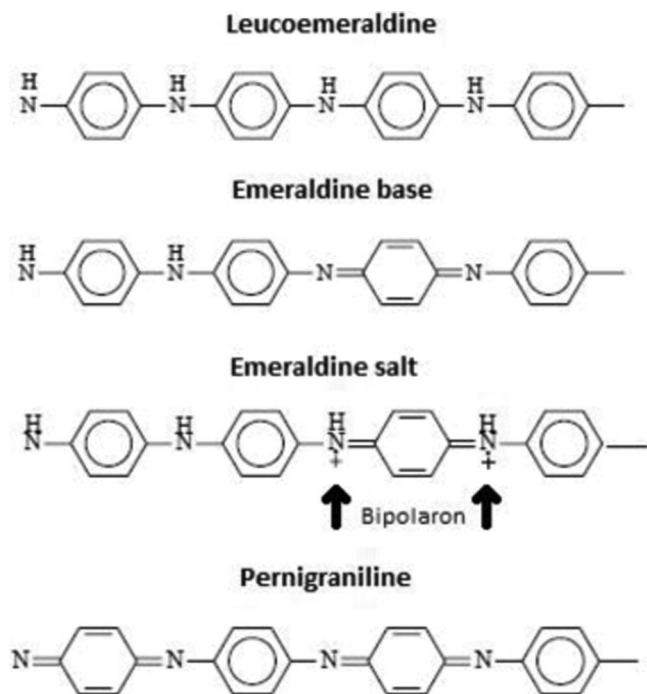


Figure 1. General scheme of fundamental oxidation forms of PANI.⁷

end. General scheme of PANI of fundamental oxidation forms are in Fig. 1.²

Other relevant material is carbon fiber felt (CFF). In 1950's, materials based in carbon fiber showed specific resistance to traction 30 times more than metal-based materials, enabling better performance in mechanical properties and weight decreasing, as required by aerospace industry.¹¹

PANI and CFF united show singular properties due to synergism existing between these materials, because the electroactive character of polymers added to high superficial area and mechanic support of CFF.¹² So, PANI@CFF composite is promisor to attend cited requirements.

In the present paper, PANI was obtained as a micrometric film grown fibers of CFF electrodes by electro-synthesis, using cyclic voltammetry. The beginning stage is very important because it is related with the quality of former layer of polymer obtained on surface, since it depends of scanning parameters. These scan numbers are studied here to a CFF annealed at set temperature.

Experimental

PANI electro-synthesis was carried by oxidative polymerization in 0.1 molL⁻¹ aniline/0.5 molL⁻¹ H₂SO₄ acid electrolyte solution.

In electrochemical cell, electrodes used were: work, CFF annealed at 1600 K in a tubular oven with continuous flow of Argon; auxiliary of Pt mesh; reference of Ag/AgCl. Prior to electrochemical process, it was performed bubbling of ultra-pure nitrogen (N₂, 99.999%) and mechanic stirring, to remove solved air. The polymerization was controlled by the cyclic application of potential from -0.50 V to + 1.05 V vs Ag/AgCl, at 25 mV s⁻¹.

Morphologic characterization of films was obtained from high resolution field emission gun scanning electron microscopy using a TESCAN MIRA3 equipment. Crystallographic structures of films were determined using X-ray diffractometer Panalytical XPertPRO, with a rotating anode X-ray generator working at 5° ≤ 2θ ≤ 90°, with Cu monochromatic radiation (0,154 nm) and spinning of samples. Electrochemical Impedance Spectroscopy (EIS) characterization was performed through Autolab PGSTAT 302 potentiostat-galvanostat, using same three electrode cell above cited. Measurements were per-

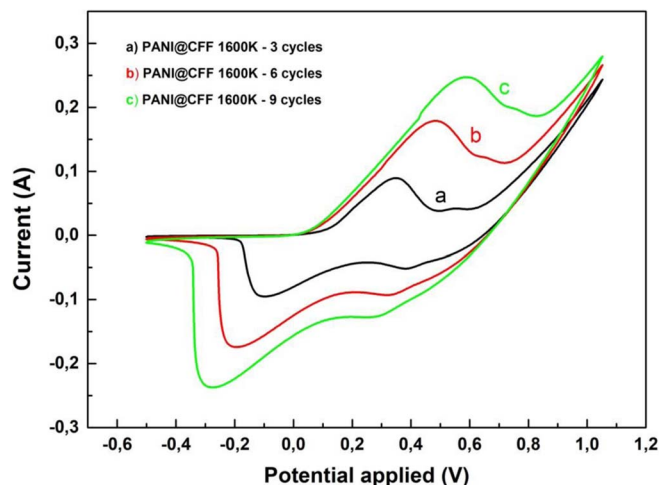


Figure 2. Polarographic data obtained during electro-synthesis of polyaniline on carbon fiber felt as substrate.

formed at open circuit potential (OCP), varying frequency from 0,1 up to 10000 Hz and potential perturbation amplitude of 10 mV. Phonons and functional groups, specially polaronic structures were determined by Raman Scattering Spectroscopy using Horiba Scientific Labram HR Evolution equipment with green laser (514.5 cm⁻¹), and Fourier Transform Infrared Spectroscopy (FT-IR) using a Perkin Elmer Spectrum Onespectrometer, with transmission by KBr pads technique.

Results and Discussion

Polarographic data.—Figure 2 shows curves of electric current in function of the potential during cyclic voltammetry experimente used to obtain layers of polyaniline on substrate (CFF). The third, sixth and ninth cycles are presented in plot, showing an increase of current of peak and separation between anodic and cathodic potential to oxidative polymerization of aniline. In fact, it is noticed that occurs a growth of PANI layer on anode (positive potential) and on cathode (negative potential). Therefore, by these data, it can be noticed that the peak potentials separates cycle by cycle, showing an increase of irreversibility of process. The current increase indicates that more polymer is formed at each cycle, and it can be waited a material more and more electroactive and possibly conductive. Nine cycles seems to be not enough to exhaust aniline content of cell, but show an increase of mass, conductivity, regular kinetics, irreversibility of process and change of composition.

It is very important to observe that, for the same surface, subject to same sweep rate, switching potential and other physicochemical factors, normally, it is expected to maintain the material composition, increasing mass of formed layer. In this electro-synthesis, there is an important shift of anodic and cathodic potential, indicating some important change of surface, and, so, variation of composition in the polymer formed. Distinct attention is gave to oxidation degree of polyaniline and its electroactivity, represented by counts of charge carriers (polarons and bipolarons). Both of properties are related to chemical composition and they are detectable by spectroscopic techniques.

It can be useful to justify this change, because it is uncommon to shift potential to same degree of oxidation. It is noticeable to former cycles, at anodic branch, two voltammetric peaks: the first, at 0.35 V, and the second, at 0.55 V. Two peaks correspond to two oxidation processes, and to polyaniline, it is related, firstly to emeraldine formation, and secondly to pernigraniline formation. The change in oxidation degree provides loss of electrons in the molecular structure, so as to produce a change in crystallographic structure, as seen in Figure 5, below. As cycles are processed, the first peak is shifted to more positive potential and convoluted with the second indicating that two

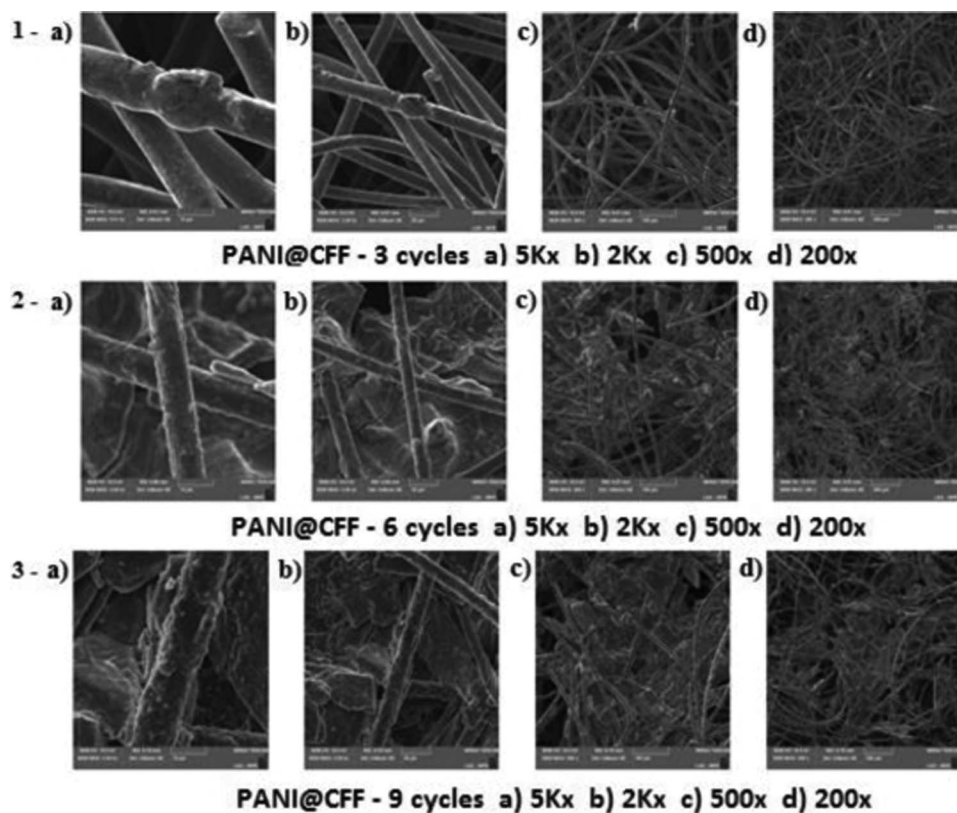


Figure 3. FEG-SEM images of PANI@CFF composite at 1) three, 2) six and 3) nine voltammetric cycles.

oxidations occur simultaneously. On the 9th cycle, the potential of oxidative polymerization is 0.59 V, greater than second potential to 3rd cycle. So, this fact can be indicating that a new model for the growth of PANI, since that potential change indicates Gibbs energy change, possibly related to surface change. It is understandable because after some number of cycles to this sweep rate, the growth of PANI on CFF substrate competes with the growth of PANI on PANI. This hypothesis can be confirmed by morphologic and structural techniques.

HR-FEG-SEM.—In the Literature,¹³ several morphologic types of PANI are cited, according to type of synthesis process and parameters. Some of them are “coral reefs”, alveolus clusters, nanofibers or plates. As shown in Fig. 3, carbon fiber felt show tubular, long form and randomly distributed. In addition, PANI appears as clusters and plates, with many porous, which cover fibers totally or partially. Figures 3.1a–3.1d shows SEM images with several magnifications of PANI@CFF composite obtained using three voltammetric cycles. This composite presents a noticeable quantity of uncovered CFF and a little bit alveolus of PANI. These morphologies evolved to agglomerated clusters showed at Figures 3.2a–3.2d, related to six voltammetric cycles. Furthermore, it is possible to verify that PANI obtained with nine voltammetric cycles (Figures 3.3a–3.3d) shows overlapped layers of PANI, as reported in the Literature,¹⁴ which represents layer of PANI growing up on PANI.

Comparing Figs. 3.1, 3.2 and 3.3, it is possible to observe that increasing voltammetric cycle number to increase the growth of PANI on CFF surface, as well as, between fibers.

X-ray diffraction patterns.—From XRD patterns, it was possible to analyze crystalline structure. According to Figure 4, carbon fiber felt presents band located at $2\theta = 26^\circ$, referent to 002 plane of carbon, attributed to hexagonal graphitic structure, with high disorder degree, observed by width of this band.⁹

PANI diffraction peaks appear around $2\theta = 6.3^\circ, 9.2^\circ, 14.7^\circ, 20.7^\circ, 25.2^\circ$ and 26.9° ,^{10,15} related to emeraldine when it has orthor-

ombic structure.¹⁶ However, most of the references available in the literature concerning the formation of the crystallographic structure of polyaniline do not mention the formation of peaks in all the orientations described. They may depend on the doping medium, the form of the synthesis and other physico-chemical parameters used in the processing system. A little quoted orientation, at 6.3° , is widely discussed by Jin et al.¹⁷ The appearance of such a peak is associated with the increase of the molar ratio between aspartic acid and aniline in the chemical synthesis of polyaniline of tetragonal structure, to specific use in electrochemical biosensors, using glassy carbon as substrate, for the determination of dopamine. Recent determinations of structure have been performed on PANI@graphene composite electrosynthesized, but the polymer obtained has clearly amorphous characteristics.^{18–20}

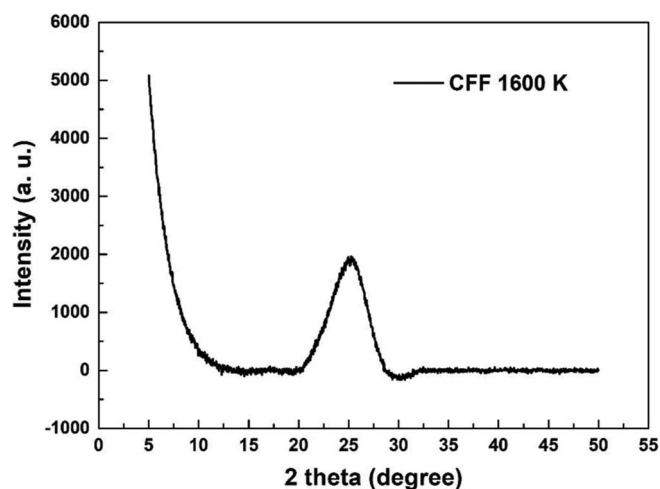


Figure 4. X-ray Diffraction of carbon fiber felt annealed at 1600 K.

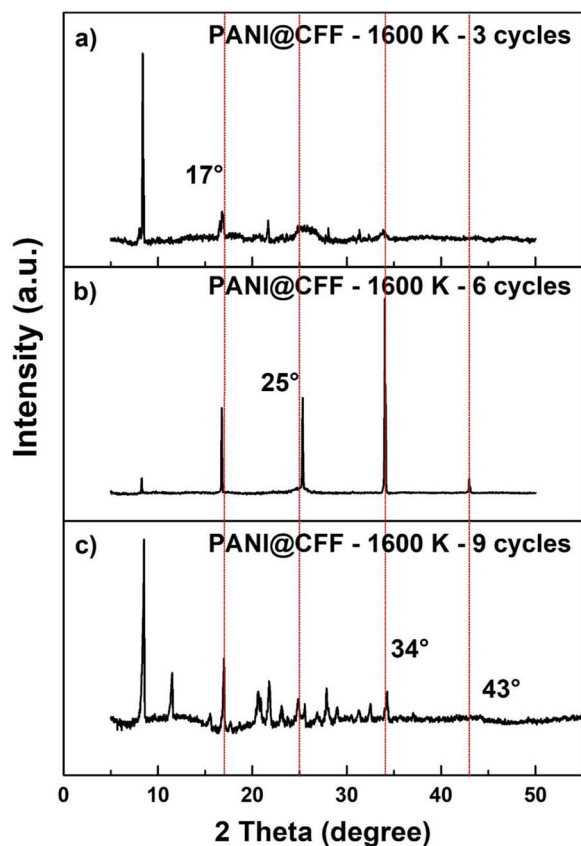


Figure 5. XRD patterns of PANI@CFF composite obtained at a) three, b) six and c) nine voltammetric cycles.

In any case, the peaks or bands presented are always consistent with some orientation found in the literature, however, with variations to the processing conditions. In this case, the analysis of diffractograms as a function of voltammetric cycles of electrosynthesis was not found and it follows according to the following paragraphs.

According to Figure 5, it is possible to observe that peculiar peaks of PANI and CFF are present in composite spectra, showing that polyaniline are covering carbon fiber felt surface.

To PANI@CFF composite obtained using three voltammetric cycles (Figure 5a), it was possible to obtain monocrystal structure of polyaniline. It can be justified by crystalline structure of fiber (parallel sheet to (002) orientation) to guide the growth of PANI (001), obtained at $2\theta = 9.4^\circ$.²¹ This data is coherent with previous showed at Figure 3.1, where is revealed formation of a little bit alveolus of PANI on CFF surface. To PANI@CFF composite obtained with six voltammetric cycles, it is difficult to detect CFF from the XRD diffractogram (Figure 5b). This contribution is over ridden by others, common to PANI, arising by diverse orientations, namely located at 17° , 25° and 34° . Less intense contribution appears at 43° . These data are supported by the appearance of planar structures related to this treatment, as reported in Figure 3.2. On the other hand, with nine voltammetric cycles (Figure 3.3), the micrographs show plates and sheets of PANI, however, less ordered on and between the CFF. Showing a growth of PANI on PANI, previously formed, creating barriers into porous structure. It is possible to associate greater variety of orientations, as shown by multiplicity of peaks in the diffractogram reported in Figure 5c.

From the XRD pattern, six voltammetric cycles revealed more intense and narrow peaks in relation to three and nine voltammetric cycles. PANI@CFF composite (formed in six voltammetric cycles) shows more regular distribution of peaks and greater crystalline definition in respect to others. It is coherent with FEG-SEM images

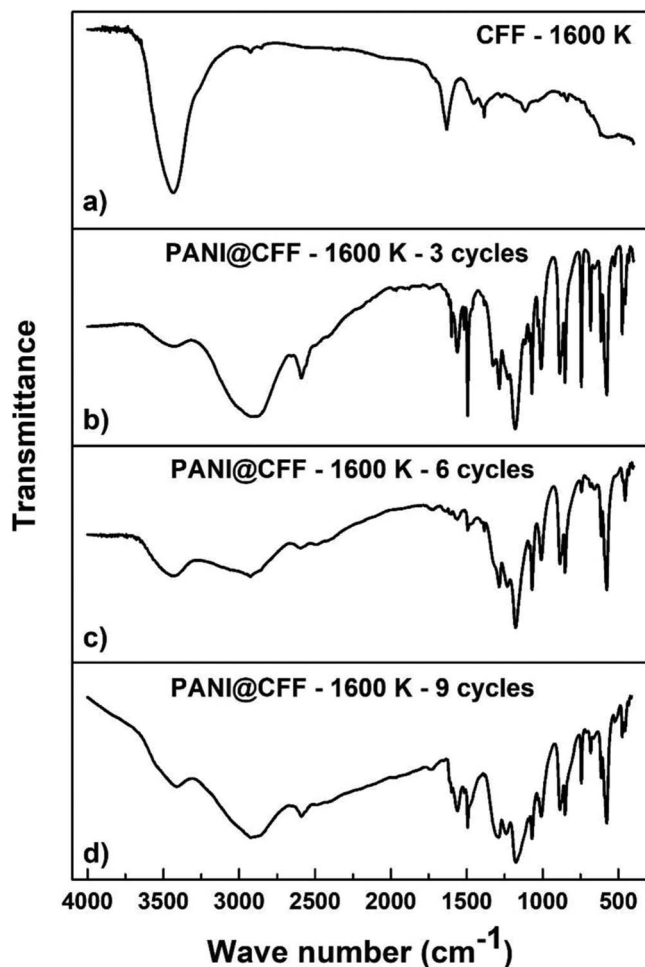


Figure 6. FT-IR spectra obtained for a) carbon fiber felt annealed at 1600 K and PANI@CFF composite at b) three, c) six and d) nine voltammetric cycles.

(Figure 3), which show more intense and homogeneous distribution of the polyaniline on carbon fiber felt.

Fourier transform infrared spectroscopy.—Fourier Transform Infrared (FTIR) spectroscopy was used to verify changes on chemical structures involved in composite formation of PANI@CFF. Figure 6 shows PANI@CFF composite spectra obtained to three, six and nine voltammetric cycles. It is possible to verify that six and nine voltammetric cycles exhibit more similar spectra when compared to three voltammetric cycles spectra.

The main contributions for all the voltammetric cycles can be observed in Table I, which was divided according to IR regions.

At 4000 to 1800 cm^{-1} region, it was observed large and intense band, related to O-H stretching. This contribution is common in the analysis using KBr pads, highly hygroscopic.²² Therefore, a band attributed to N-H stretching, common to PANI and other aminic polymers, is also observed between 3750 and 3250 cm^{-1} , as can be noticed at Table I.

In the first region of MIR (Middle Infrared) (Figure 7), 1600–1450 cm^{-1} , there are two bands located at 1564 and 1494 cm^{-1} , attributed to C=C stretching at quinoid and benzenoid, respectively. In both cases, identified structure is partially reduced in relation to emeraldine state, suggesting intermediate structure formation between protoemeraldine and emeraldine²³ possibly due to cycles end at cathodic potential. PANI formed at three voltammetric cycles seems to be less oxidized between them. Raman scattering spectroscopy (Figure 10) seems to be more precise to this assert, since transmission technique is just semi quantitative.²⁹

Table I. Main bands obtained by FT-IR.

Bands	Atributions	References
3460 and 3380 cm^{-1}	Assimetric and simetric streching N-H at NH_2 groups.	22
3380–3388 cm^{-1}	N-H streching at B–NH–B	22,25,28
3310–3290 cm^{-1}	NH streching	22,25,28
3170–3257 cm^{-1}	Terminal Q = NH streching	22,25,28
1600–1450 cm^{-1}	N-H deformation. C=N stretching, aromatic ring	18
1565–1595 cm^{-1}	C=C stretching in quinoid ring structure(N=Q=N) in aniline oligomers	22,23
1510–1490 cm^{-1}	C=C stretching in benzenoid ring (N-B-N).	22,24
1400–1240 cm^{-1}	C-N stretching to aromatic amines	23
1380–1374 cm^{-1}	C-N stretching to Q-B _{trans} -Q	22
1315–1305 cm^{-1}	C-N stretching to Q-B _{cis} -Q, QBB, BBB sequences(favors partially electroactives functionalities)	23,25
1240–1255 cm^{-1}	C-N stretching in BBB sequence (unfavors electroactivity)	23
1220–500 cm^{-1}	C-H bending in aromatic rings in or out of sheet	26
1170–1140 cm^{-1}	Vibrational mode Q = NH^+ -B or B- N^+ H-B (semiquinoid polaronic structure – typically conductive – first of them being more conductive)	22,27
850–854 cm^{-1}	Substitution 1,2,4 of benzenic ring	22
740–766 cm^{-1}	Substitution 1,2 or mono-substitution	22

At next region (Figure 8), 1240–1400 cm^{-1} , bands associated to distribution of oxidation forms and it be repeats as three some at chain appear, high lighting C-N stretching. Structures where quinoid and benzenoid are in sequence, such as for example, Q-B_{trans}-Q, Q-B_{cis}-Q, QBB, or BBQ favor partially electroactivity, since polaronic structure generation is related to the alternance between quinoid and benzenoid structures. In a particular way, Q-B_{trans}-Q structure tends to linearize molecule in such way to order effectively and comes back more crystalline supposing predomination in chain.²⁹ Theoretically, BBB structures unfavor conductivity, because it corresponds to leucoemeraldine structure, which does not show thermodynamic condition to supplant bandgap. Very discreet is the record of QB_{trans}Q

structures, using three and six voltammetric cycles, reported at 1385 cm^{-1} . Noticeable is doublet formed around 1300 cm^{-1} , which degenerate in band from three up to nine voltammetric cycles, indicating transitions from semiquinoid to benzenoid structures, being 1281 cm^{-1} band more pronounced in three voltammetric cycles spectrum (Figure 8b), indicating material with less degree of oxidation and a few points of electric charge accommodation. This number decreases with voltammetric cycles treatment, probably because extinction of chemical potential of system and process ending cathodic potential.

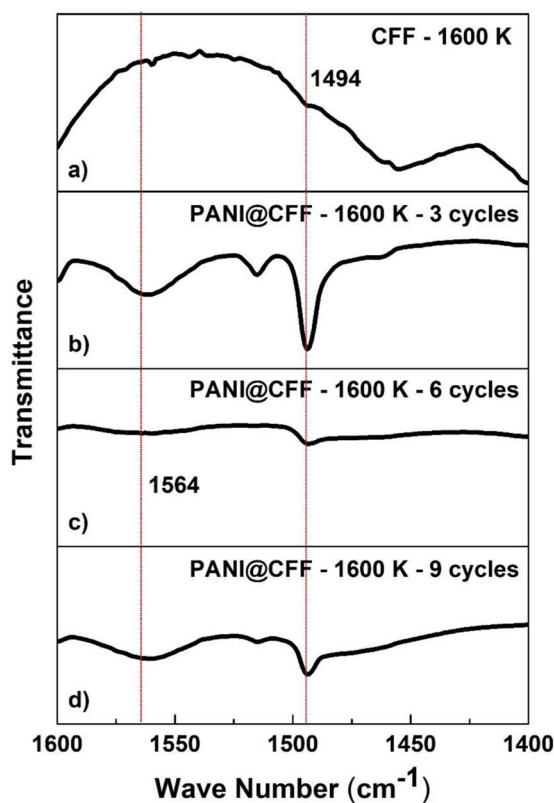


Figure 7. Partial FT-IR spectra of a) carbon fiber felt annealed at 1600 K and PANI@CFF composite obtained at b) three, c) six and d) nine voltammetric cycles in interval 1600–1450 cm^{-1} .

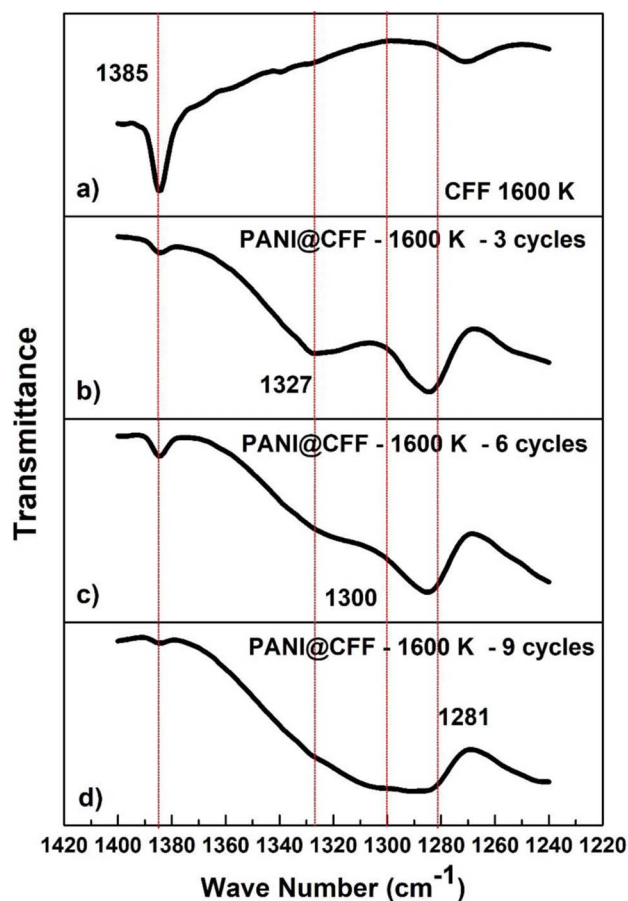


Figure 8. Partial FT-IR spectra of a) carbon fiber felt annealed at 1600 K and PANI@CFF composite obtained at b) three, c) six and d) nine voltammetric cycles in interval 1400–1240 cm^{-1} .

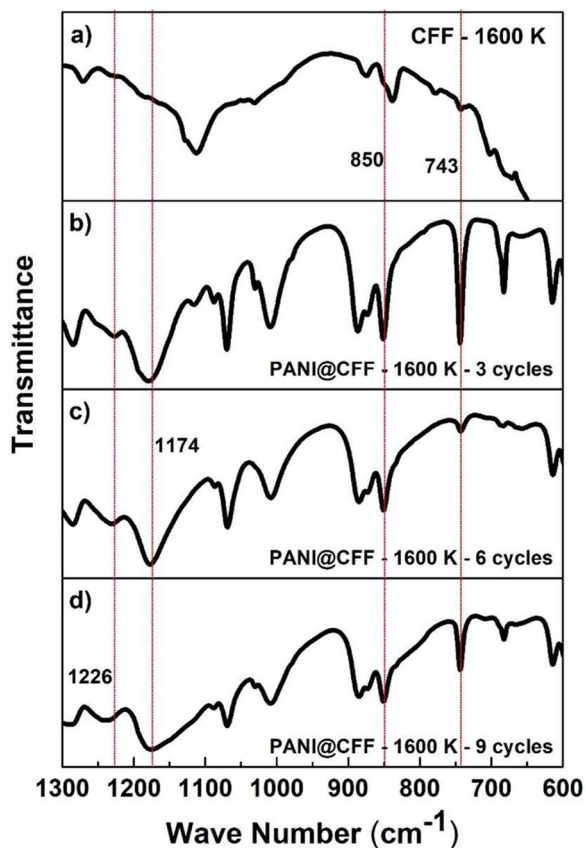


Figure 9. Partial FT-IR spectra of a) carbon fiber felt annealed at 1600 K and PANI@CFF composite obtained at b) three, c) six and d) nine voltammetric cycles in interval 1200–600 cm^{-1} .

However, gradual disappearing of 1327 cm^{-1} band or its degeneracy in convolution with 1281 cm^{-1} band indicates possible decreasing in conductive electroactivity of PANI, enabling condition to form more capacitive material.

The third interval (Figure 9) is directly related to IR signal of charge carriers, which enable more effectively some asserts concerning to conductivity. There are important and significant bands at 1226 cm^{-1} (1,4-substitution in benzenic ring, contributing to chain linearity and orientation) and 1174 cm^{-1} (related to vibrational mode $Q = \text{NH}^+ - \text{B}$ or $\text{B} - \text{N}^+ - \text{H} - \text{B}$).²⁵ Band referent to 1,4-substitution highlights more with more extended (nine voltammetric cycles, Figure 9d), indicating chain linearization with electrochemical cycles. This effect can be associated to decreasing of presence of structure 1,2-substitution (whose intensity decreases a lot at 743 cm^{-1} – 1,4-substitution in aromatic ring followed by loss of band intensity at 850 cm^{-1} – 1,2,4-substitution in aromatic ring). To 1174 cm^{-1} band, all samples of PANI@CFF composite (three, six and nine voltammetric cycles) shows electroactive contribution, enabling charge placing in structure and indicating possibilities to assert doping. Bands have variable width, symmetry and intensity, being less intense, more large and asymmetric obtained with nine voltammetric cycles, which can be indicate lower tendency to place electric charge enabling charge dissipation. To three (Figure 9b) and six (Figure 9c) voltammetric cycles, both bands are noticeably intense, and more narrow to six voltammetric cycles. This behavior is coherent with the Literature^{30–32} associating crystallinity to conductivity. Therefore, three and six voltammetric cycles can provide more capacitive composite, while six and nine voltammetric cycles treatments seem more suitable to EMI filters, since, from 6th cycle, structure rearrangement occurs, according to XRD patterns (Figure 5), gaining conductive character (dissipating charges more easily, as it happens when bipolaron structure prevails).

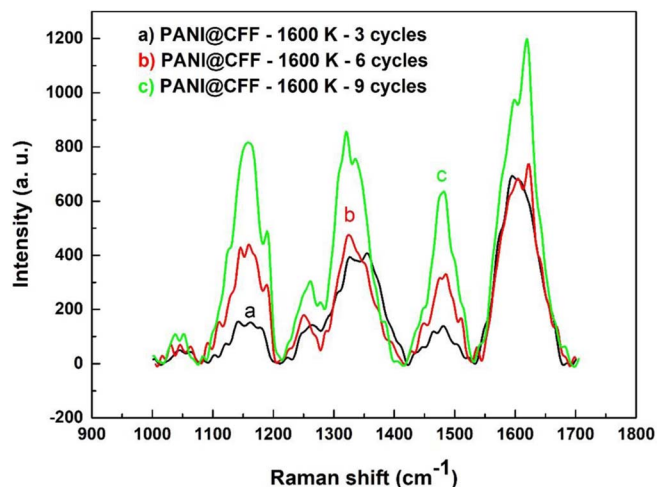


Figure 10. Raman spectra of PANI@CFF composite obtained at 3, 6 and 9 voltammetric cycles.

Raman scattering spectroscopy.—By Raman spectroscopy, it was possible quantify some attributions ratio, already qualitatively verified by FT-IR. Obtained spectra are in Figure 10. It was possible to deconvolute all band contributions to spectra formation. To this end, Gaussian functions were more suitable.

Contributions can be associated to phonons described at Table II.

According Table II, it is possible to calculate several properties of PANI@CFF composite, such as oxidation degree and an index related to material conductivity.

To determine oxidation degree (y), ratio of intensities attributed to C=C stretching at quinoid rings in relation to C=C stretching at whole PANI quinoid and benzenoid rings were calculated. As shown at Figure 1, $y = 0$ corresponds to leucoemeraldine, $y = 0.5$ corresponds to emeraldine, and $y = 1.0$ corresponds to pernigraniline. In this way, y can be calculated using the Equation 1:

$$y = \frac{I_Q}{I_Q + I_B}, \quad [1]$$

where I_Q is related to C=C stretching quinoid form peak intensity, and I_B is the same related benzenoid oxidaton form.

Furthermore, to determine a conductivity index (S), it can be compared intensity of contributions of polaron ($\text{C} - \text{N}^+$) and bipolaron ($\text{C} = \text{N}^+$). Polarons are electrically actives, but bipolarons contribute more effectively to conductivity phenomena. The formers confer capacitive effects, but the lasts provide electroactive versatility to material. Therefore, it is possible to calculate this index through ratio between intensities of bands related to positive nitrogen (imine and amine, respectively) charged (in this way, a hole) at bipolaron (I_{BP}) and polaron (I_P) structures, as shown in Equation 2.

$$S = \frac{I_{BP}}{I_P} \quad [2]$$

Using Equations 1 and 2 on band deconvolution data of spectra of Figure 10, the Table III is generated.

From Table III, increasing of voltammetric cycle numbers provides evolution of structure from leucoemeraldine ($y = 0$) to emeraldine ($y = 0.5$). Emeraldine provides higher quantity of states to place charges carriers in its chain. This fact explains increased bipolaron quantity versus cycle number, around ten times from three to nine voltammetric cycles. This behavior indicates that the conductivity index of PANI@CFF composite increases from 0.015 to 0.122, for three and nine voltammetric cycles, respectively. As discussed at item 3.1, the growth of PANI on PANI justifies a very important change of composition, because the surface of CFF is different cycle by cycle.

Table II. Raman bands to PANI@CFF composite.

Raman Shift (cm ⁻¹) – 3 Cycles	Raman Shift (cm ⁻¹) – 6 Cycles	Raman Shift (cm ⁻¹) – 9 Cycles	Attribution	References
1043–1085	1016–1091	1035–1082	C–H deformation at aromatic ring	32, 33
1141–1162	1145–1169	1141–1163	C–H deformation at quinoid structure of emeraldine	32, 34, 35
1181	1190	1191	C–H deformation at leucoemeraldine salt	32, 34, 36
1222–1244	1224–1251	1237–1251	C–N stretching in amines of emeraldine	32, 33, 36, 37
1264		1262	D4 – related to carbon structure asymmetries	38
1291–1377	1271–1375	1273–1371	C–N ⁺ at polaronic forms	32, 34, 36, 37
1354	1350	1371	D1 – related to carbon structure asymmetries	32, 34, 37
1392–1433	1393–1428	1385–1442	C–C stretching at quinoid	32, 34, 36, 37
1446–1481	1446–1491	1448–1482	C=N (imine) stretching at emeraldine base	32, 34, 33, 37, 39
1505	1512	1501	D3 – related to carbon structure asymmetries	38
			C=N ⁺ stretching at bipolaronic forms and secondly N–H deformation	34, 37
1523	1536	1514	N–H deformation/C–C stretching at benzenoid	32, 33
1551–1570	1568	1540	G band – symmetric structure of CFF carbon lamellas	
1589	1591	1600	C=C stretching quinoid form	32, 33, 36
1607	1607	1575	D2 – related to carbon structure asymmetries	
1661	1669	1639	C=C stretching at benzenoid form	32, 33, 37
1612–1640	1622–1629	1620		

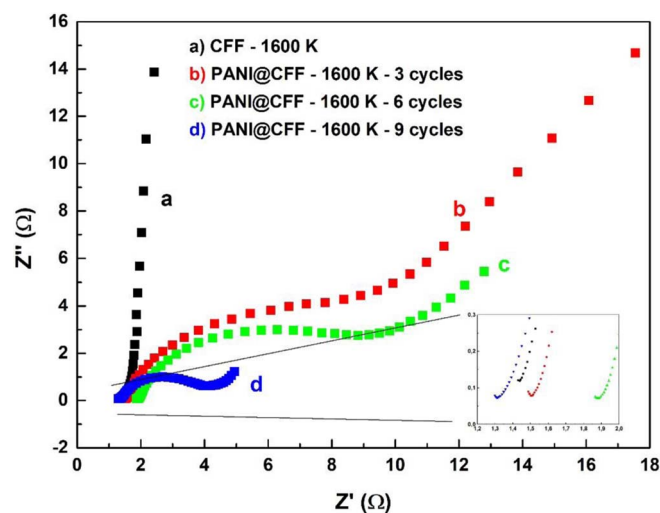
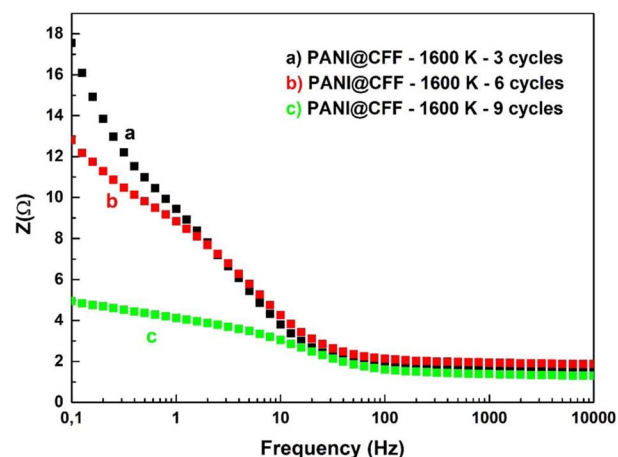
Table III. Oxidation degree and conductivity index of PANI@CFF composites obtained with three, six and nine voltammetric cycles.

Electrochemical cycle numbers	<i>y</i>	<i>S</i>
3	0.022	0.015
6	0.181	0.051
9	0.379	0.122

Electrochemical Impedance Spectroscopy (EIS).—Electrode process can be related to electric circuit components through Electrochemical Impedance Spectroscopy.^{12,41} Figure 11 shows Nyquist plot of PANI@CFF composite to three, six and nine voltammetric cycles and carbon fiber felt annealed at 1600 K.

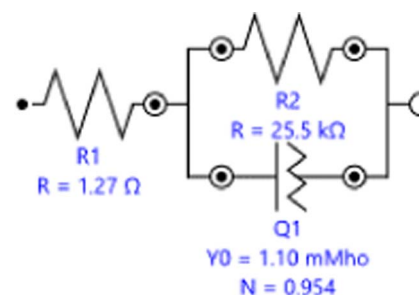
According to Nyquist (Figure 11) and Bode Modulus plots (Figure 12), it is noticeable that CFF shows impedance higher than PANI@CFF composite,¹² especially at low frequency between 0.1 and 100 Hz.

Nyquist Plot for CFF (Figure 11a) shows high impedance behavior of Helmholtz double layer, mostly capacitive, accumulating high quantity of charge and hampering electric current. In Figure 11b, the

**Figure 11.** Electrochemical Impedance Spectroscopy of carbon fiber felt annealed at 1600 K and PANI@CFF composite obtained at 3, 6 and 9 voltammetric cycles.**Figure 12.** Bode modulus of PANI@CFF composite obtained at 3, 6 and 9 voltammetric cycles.

slope of the Nyquist plot decreases considerably after 3 cycles due to the formation of polarons and bipolarons, as can be inferred from the data in Table III. This same Figure shows that there is a decrease associated with the formation of other phases for the higher cycle numbers: 6 (Figure 11c) and 9 (Figure 11d), following the general downward trend in impedance. Moreover, the effect of the fiber surface becomes less noticeable in order to privilege the detection of effects of the PANI surface. Equivalent circuit shows common characteristics of carbon electrodes, as shown in Figure 13.

In a general way, circuit behavior follows Literature models.⁴² Figure 13 show equivalent circuit of electrode obtained from three,

**Figure 13.** Equivalent circuit of CFF electrode annealed at 1600 K.

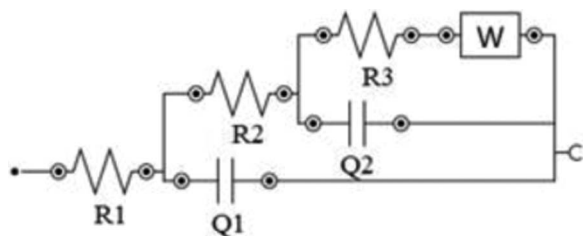


Figure 14. EIS circuit fit of PANI@CFF composite.

six and nine voltammetric cycles of PANI@CFF electrosynthesis, based in NLLS method (Non Linear Least Square) to fit spectra of Figure 11,^{43,44} through software NOVA 1.11.2.

Figure 14 shows EIS circuit fit of PANI@CFF composite, where R1 represents the solution ohmic resistance; Q1 and R2 represents charge accumulation on interface solution/PANI@CFF on external electrode region, and its charge transfer resistance, respectively; Q2 and R3, charge accumulation on interface solution/PANI@CFF in inner electrode regions and its resistance, respectively. Therefore, W (Warburg impedance – Y_w is Warburg admittance) reports semi finite diffusion inside CFF or PANI@CFF surface, by concentration gradient of species. For circuit obtained with 9 cycles, the authors considered $Q1 = CPE = 0.769$ (constant phase element). These last elements are related to behavior of capacitive, resistive and diffusive effects which occur directly on each fiber of CFF. So, the growing of PANI and changes in its morphologic, structural, chemical and electric properties imply firstly on variations occurred Q2, R3 e Y_w .

It is important to remember that EIS technique provides information to analyze the effects of electrode material on Helmholtz double layer formed around it. This analysis considers, as well the all electrode as, its parts, being porous and tridimensional. This approach was used to similar materials by Dalmolin et al.,^{3,42} where cycle counts modified material structure and morphology, as earlier observed, such as change behavior of surface interactions. They do not follow linearly material bulk properties. However, they are influenced by relevant modification of electric effects on Helmholtz double layer, indicated at Table IV.

According to Table IV, solution resistance decreases for PANI@CFF composite obtained at nine voltammetric cycles after the increase to six voltammetric cycles. Between three and six voltammetric cycles, observed through Figure 3, there is a variation in the way of growth of PANI from “on fiber” to “between fibers”. This configuration can offer impedance behavior differentiated among them (Figure 11). The capacitive effects on PANI@CFF composite obtained at three voltammetric cycles is due to incipient PANI particles formed on CFF surface. To six or more voltammetric cycles, the original pores on carbon fiber felt surface are not completely available to transport. And the effects measured by EIS have other meanings. It is very important to pay attention to low frequency phenomena, normally found in more internal circuit elements and measured at right

Table IV. Circuit elements obtained from EIS circuit fit of PANI@CFF composite obtained at 3, 6 and 9 voltammetric cycles.

	3 cycles	6 cycles	9 cycles
R1 (Ω)	1.27	1.85	1.31
R2 (Ω)	0.213	4.83	2.85
Q1 (mF)	0.028	4.97	*
R3 (Ω)	3.0	0.799	0.239
Q2 (mF)	3.79	16.5	332
Y_w (mMho)	70.6	179	938
χ^2	0.03	0.003	0.02

*This CPE indicates that a resistance is associated to this capacitive behavior, showing an admittance of 11.3 mMho and a phase exponent of 0.769.

side of Nyquist Plot, and related to microstructural and morphologic properties of surface of substrate.

From Figure 3, it is noticeable that polyaniline forms a barrier to charge and mass transport. Limited number of charge carrier structures hinders mass transport, so increasing diffusive parameter Y_w , and causing an appearing of capacitive effect, increasing Q2 in two orders of magnitude. Therefore, these effects are combined with decrease of R3, in one order of magnitude, that can indicate a more conductive layer between fibers of CFF, inevitably related to increase and change of properties of PANI formation. It can be associated to significant increasing of number of charge carriers, from three up to nine voltammetric cycles. Due to excess of surface bipolaron on PANI@CFF composite obtained at nine voltammetric cycles, charges are partially unleashed from material to double layer or to solution. In fact, Raman spectroscopy appointed that a very important increasing of bipolarons occurred. However, this movement is very suitable to capacitive systems, since that promotes as accommodation as transport of electric charge.

All of them phenomena are followed by consumption of charges registered by variation of Randles circuit properties. The high organization registered by XRD can be related to limited transport of electric charge to six voltammetric cycles. This property was observed by Figure 5, where is noticeable very high definition of PANI peaks. This relation suggests to authors that six voltammetric cycles is an important milestone to change of regime of growth of PANI on CFF substrate. The highest value of R2 is found to six voltammetric cycles and indicates the lowest rate of polymerization of aniline on CFF. From this observation, the authors claims that, CFF annealed at 1600 K, it is very important to exceed six voltammetric cycles to produce a suitable electroactive composite, mainly if the goal is related to facile storage and transport of electric charge. After that, to grow PANI on PANI, the process turns to give a preferential orientation at $2\theta = 9.2^\circ$, increasing parallel plates effect inner to PANI structure, which is typical to capacitors. Clearly, changes on annealing of CFF require a systematic study to assert such relationship.

However, all of these properties can be combined with a minimal over oxidation process. For carbon fiber felt, nine voltammetric cycles are not enough to do it, and more cycles could be applied without offer this additional problem. It can be useful to study the behavior of PANI@CFF composite material in a supercapacitor cell, to evaluate its stability in a prototype.

Conclusions

PANI@CFF composite was electrochemical synthesized through three different number of voltammetric cycles, which provided structural evolution from leucoemeraldine to emeraldine. Because emeraldine salt to be more enable to place bipolaron, conductivity increases versus number of voltammetric cycles. For nine voltammetric cycles, due to more available bipolaron, it occurs more charge transference, releasing charges to Helmholtz double layer and to solution, being a better charge dissipater. It was indicated by FT-IR, through large and asymmetric bands, related to un-specific contribution to this behavior, and confirmed by Raman spectroscopy.

Crystallinity was also allowed in this paper, showing that number of voltammetric cycles provided evolution from monocrystalline to polycrystalline, especially after six voltammetric cycles. This stage is associated to a rearrangement of structure, which provided redistribution of charges in electrochemical cell.

Nine voltammetric cycles composite is more conducting composite PANI@CFF, originating interfaces more electroactive, by increasing as well in accumulation as in unleashing of electric charge from material to electrolyte environment.

Acknowledgments

Authors thanks to technicians of AMR/IAE and LAS/INPE, and Financial Support of FAPESP (grant number 16/11462-3 and CNPQ (grant number 136184/2016-2)).

References

1. A. G. MacDiarmid, "Synthetic Metals: A novel role for organic polymers (Nobel Lecture)," *Angew. Chem.*, **40**, 2581 (2001).
2. R. Ramkumar and M. M. Sundaram, "Electrochemical Synthesis Of polyaniline cross-linked NiMoO₄. nanofiber dendrites for energy storage devices," *New J. Chem.*, **40**, 7456 (2016).
3. C. Dalmolin, S. C. Canobre, S. R. Biaggio, R. C. Rocha-Filho, and N. Bocchi, "Electropolymerization of polyaniline on high surface area carbon substrates," *Journal of Electroanalytical Chemistry*, **578**, 9 (2005).
4. A. Kausar, "Electromagnetic interference shielding of polyaniline/Poloxalene/carbon black composite," *International Journal of Materials and Chemistry*, **6**(1), 6 (2016).
5. P. Nunziante and G. Pistoia, "Factors affecting the growth of thick polyaniline films by the cyclic voltammetric technique," *Electrochimica Acta*, **34**(2), 223 (1989).
6. C. Q. Cui, L. H. Ong, T. C. Tan, and J. Y. Lee, "Origin of the difference between potentiostatic and cycles potential sweep depositions of polyaniline," *J. Electroanal. Chem.*, **346**, 477 (1993).
7. C. Q. Cui, L. H. Ong, T. C. Tan, and J. Y. Lee, "Extent of incorporation of hydrolysis products in polyaniline films deposited by cyclic potentials weep," *Electrochimica Acta*, **38**(10), 1935 (1993).
8. G. T. Andrade, M. J. Aguirre, and S. R. Biaggio, "Influence of the first potential scan on the morphology and electrical properties of potentiodynamically grown polyaniline films," *Electrochimica Acta*, **44**, 633 (1998).
9. J. L. Bredas and G. B. Street, "Polarons, Bipolarons, and Solitons in conducting polymers," *Acc. Chem. Res.*, **18**(10), 309 (1985).
10. P. w. Anderson, "Model for the electronic structure of amorphous semiconductors," *Phys. Rev. Lett.*, **34**(15), 953 (1975).
11. E. Radovanovic, Utilização de polímeros de silício como precursores de SiC e SiC_xO_y na obtenção de compósitos contendo Fibras de Carbono. *Thesis, Universidade Estadual de Campinas*, Campinas, 2000.
12. L. L. Souza, Uso da Voltametria Cíclica e da Espectroscopia de Impedância Eletroquímica na Determinação da Área superficial ativa de Eletrodos Modificados a Base de Carbono. *Thesis, Instituto de Pesquisas Energéticas e Nucleares Associada a Universidade de São Paulo*, São Paulo, 2011.
13. D. Chao, J. Chen, X. Lu, L. Chen, W. Zhang, and Y. Wei, "SEM study of the morphology Of high molecular weight polyaniline," *Synthetic Metals*, **150**, 47 (2005).
14. K. Tzou and R. V. Gregory, "Kinetic study of the chemical polymerization of aniline in aqueous solutions," *Synthetic Metals*, **47**, 267 (1992).
15. L. R. Oliveira, L. Manzato, Y. P. Mascarenhas, and E. A. Sanches, "The influence of heat-treatment on the semi-crystalline structure of Polyaniline Emeraldine-salt form," *Journal of Molecular Structure*, **1128**, 707 (2017).
16. X. Lu, H. Dou, YANG S., L. Hao, L. Zhang, L. Shen, F. Zhang, and X. Zhang, "Fabrication and electrochemical capacitance of hierarchical graphene/polyaniline/carbon nanotube ternary composite films," *Electrochimica Acta*, **56**(25), 9224 (2011).
17. E. Jin, L. Xiaofeng, B. Xiujie, K. Lirong, Z. Wanjin, and W. Ce, "Unique tetragonal polyaniline microstructure and its application in electrochemical biosensing," *J. Mater. Chem.*, **20**, 307 (2010).
18. S. N. Mehdi and Z. Fatemeh, "Electrochemical reduced graphene oxide-polyaniline as effective nanocomposite film for high-performance supercapacitor applications," *Electrochimica Acta*, **246**, 575 (2017).
19. P. Nazish, M. Neelima, O. A. Mohd, and H. C. Moo, "Enhanced electrochemical behavior and hydrophobicity of crystalline polyaniline@graphene nanocomposite synthesized at elevated temperature," *Composites Part B*, **87**, 281 (2016).
20. J. Yaser, M. G. Sayed, and S. N. Mehdi, "Electrochemical deposition and characterization of polyaniline-graphene nanocomposite films and its corrosion protection properties," *J. Polym. Res.*, **23** (2016).
21. A. Abdolahi, E. Hamzah, Z. Ibrahim, and S. Hashim, "Synthesis of Uniform Polyaniline Nanofibers through Interfacial Polymerization," *Materials*, **5**(8), 1487 (2012).
22. E. C. Mattos, I. Viganò, R. C. L. Dutra, and M. F. Diniz, "Aplicação de metodologias FT-IR de transmissão e fotoacústica à caracterização de materiais altamente energéticos – parte ii," *Quim. Nova.*, **25**(5), 722 (2002).
23. J. Tang, X. Jing, B. Wang, and F. Wang, "Infrared spectra of soluble polyaniline," *Synthetic Metals*, **24**, 231 (1988).
24. H. Wang, X. Yang Q.Hao, L. Lu, and X. Wang, "Graphene oxide doped polyaniline for supercapacitors," *Electrochemistry Communications*, **11**, 1158 (2009).
25. E. Dmitrieva and L. Dunsch, "How linear is "linear" polyaniline?," *J. Phys. Chem. B.*, **115**(20), 6401 (2011).
26. A. L. Smith, *Applied infrared spectroscopy: fundamentals, techniques, and analytical problem-solving*, Vol. **54**, Emeritus, 1979.
27. M. A. C. Mazzeu, Estudo das Variações Estruturais e Morfológicas em função do tempo de Síntese e da Cinética de Polimerização da Polianilina. *Thesis, Instituto Tecnológico da Aeronáutica*, São José dos Campos, 2016.
28. X. R. Zeng and T. M. Ko, "Structures and properties of chemically reduced polyanilines," *Polymer*, **39**(5), 1187 (1998).
29. Ph. Colomban, A. Gruger, A. Novak, and A. Régis, "Infrared and Raman study of polyaniline: Part I. Hydrogen bonding and electronic mobility in emeraldine salts," *Journal of Molecular Structure*, **3**(17), 261 (1994).
30. J. P. Pouget, E. M., A. J. Epstein Jozefowicz, X. Tang, and A. G. MacDiarmid, "X-ray structure of polyaniline," *Macromolecules*, **24**, 779 (1991).
31. J. Vivekanandan, V. Ponnusamy, A. Mahudewaran, and P. S. Vijayanand, "Synthesis, characterization and conductivity study of polyaniline prepared by chemical oxidative and electrochemical methods," *Arch. Appl. Sci. Res.*, **3**(6), 147 (2011).
32. J. Laska and J. Widlarz, "Spectroscopic and structural characterization of low molecular weight fractions of polyaniline," *Polymer*, **46**(5), 1485 (2005).
33. R. Mazeikienė, V. Tomkute, Z. Kuodiz, G. Niaura, and A. Malinauskas, "Raman spectroelectrochemical study of polyaniline and sulfonated polyaniline in solution of different pH," *Vibrational Spectroscopy*, **44**(2), 201 (2007).
34. R. Mazeikienė, G. Niaura, and A. Malinauskas, "A comparative Raman spectroelectrochemical study of selected polyaniline derivatives in a pH-neutral solution," *Synthetic Metals*, **160**, 1060 (2010).
35. Z. Morávková, M. Tchorvá, M. Exnerová, and J. Stejskal, "The carbonization of thin polyaniline films," *Thin solid films*, **520**(19), 6088 (2012).
36. Y. Wang and JING X., "Effect of solution concentration on the UV-Vis spectroscopy measured oxidation state of polyaniline base," *Polymer Testing*, **24**(2), 153 (2005).
37. M. M. Nobrega, M. Cappatelli, M. L. A. Temperini, and R. Bini, "Pressure-induced reactivity in the emeraldine salt and base forms of polyaniline probed by FT-IR and Raman," *J. Phys. Chem. C.*, **118**(47), 27559 (2014).
38. X. Wang, M. C. Bernard, C. Deslouis, S. Joiret, and P. Rousseau, "Kinetic reactions in thin polyaniline films revisited through Raman - impedance dynamic coupling," *Electrochimica Acta*, **56**(10), 3585 (2011).
39. Yi Zhou, Z. -Y. Qin, L. Li, Y. Zhang, Y-L. Wei, L-F. Wang, and M-F. Zhu, "Polyaniline/multi-walled carbon nanotube composites with core-shell structures as supercapacitor electrode materials," *Electrochimica Acta*, **55**(12), 3904 (2010).
40. G. M Nascimento, P. Y. G. Kobata, and R. P. Millen, "M. L. A. Temperini Raman dispersion in polyaniline base forms," *Synthetic Metals*, **157**(6-7), 247 (2007).
41. J. Laska and J. Widlarz, "Spectroscopic and structural characterization of low molecular weight fractions of polyaniline," *Polymer*, **46**(5), 1485 (2005).
42. C. Dalmolin, S. R. Biaggio, R. C. Rocha Filho, and N. Bocchi, "Reticulated vitreous carbon/polypyrrole composites as electrodes for lithium batteries: Preparation electrochemical characterization and charge-discharge performance," *Synthetic Metals*, **160**(1-2), 173 (2010).
43. B. A. Boukamp, "A nonlinear least squares fit procedure for analysis of immittance data of electrochemical systems," *Solid State Ionics*, **20**, 31 (1986).
44. B. A. Boukamp, "A package for impedance/admittance data analysis," *Solid State Ionics*, **18-19**, 136 (1986).